Materials Research Proceedings **26** (2023) 207-212 https://doi.org/10.21741/9781644902431-34

On the effects of strain wave gear kinematic errors on the behaviour of an electro-mechanical flight control actuator for eVTOL aircrafts

Roberto Guida[1,a *], Antonio C. Bertolino[1,b], Andrea De Martin[1,c], Andrea Raviola[1,d], Giovanni Jacazio[1,e] and Massimo Sorli[1,f]

[1]Department of Mechanical and Aerospace Engineering, Politecnico di Torino, Torino, Italy

[a]roberto.guida@polito.it, [b]antonio.bertolino@polito.it, [c]andrea.demartin@polito.it, [d]andrea.raviola@polito.it, [e]giovanni.jacazio@formerfaculty.polito.it, [f]massimo.sorli@polito.it

Keywords: Strain Wave Gear, Kinematic Error, eVTOL Aircrafts EMA

Abstract. In recent years, the increasingly growing overcrowding of urban environments and the resulting road traffic congestion have pushed toward the search for alternative mobility solutions, among which there are novel Urban Air Mobility (UAM) technologies. The UAM, together with the development of electric actuation systems, would allow decongesting the streets by exploiting the sky using electric Vertical Take-Off and Landing (eVTOL) aircrafts. Urban air mobility vehicles are primarily based on fully electrical flight control systems with rotary output. Since such technology is relatively new and unproven, Prognostic and Health Management (PHM) algorithms, able to continuously monitor the health status of such systems, are of particular interest. The diffusion of these systems strongly depends on the general confidence of possible customers. The present paper proposes a preliminary study on the effects of the kinematic error of a Strain Wave Gear (SWG), the most used reducer for this kind of applications, on the behaviour of an Electro-Mechanical Actuator (EMA) used as a flight control actuator for an eVTOL aircraft. The simulation results show how the unavoidable kinematic error affects the EMA performances and how its presence can be detected and quantified in strain wave gears.

Introduction

Overcrowded cities and road traffic congestion, together with their problems related to environmental and noise pollution, have pushed the search for alternative mobility solutions. A possible solution to this problem is the Urban Air Mobility. This term refers to the use of urban airspace for intracity passenger transportation, package delivery, healthcare applications, and emergency services. Since environmental pollution in cities is one of the main issues of our time, UAM converged to all-electric aircrafts with compact Electro-Mechanical Actuators (cEMAs) with rotary output for both lift devices and flight controls.

Fatal accidents and low reliability were the main obstacles to previous UAM development. For this reason, and for the fact that this technology is still relatively new, the application of Prognostic and Health Management logics to this system may be a valuable and efficient solution [1]. Nevertheless, the design of novel PHM routines requires a significant amount of data representative of both nominal and off-nominal health conditions. This information can come from historical series, laboratory tests, or simulation campaigns. Although the first two options are usually preferable, they are often not feasible for newly developed systems and require a significant amount of time and monetary investment. Within this framework, researchers often rely on High-Fidelity (HF) models to generate datasets required to train PHM algorithms. In traditional EMAs, a lot of work has been done with this aim for what concerns electrical [2] and mechanical components [3,4] as well as flight control connections [5].

One of the possible actuation and control systems for UAM applications consists of a fault-tolerant brushless DC motor, a Strain Wave Gear, control and power electronics, and sensors. Despite traditional flight commands, the actuator presents a rotative output and not a linear one

Materials Research Proceedings **26** (2023) 207-212 https://doi.org/10.21741/9781644902431-34

[3]. In this kind of application, the use of SWGs is mainly justified by the need for a high transmission ratio (τ) within a small volume. This solution also presents several advantages over traditional gearboxes like very low backlash, good precision, and excellent repeatability. For these reasons, it is commonly used in robotics [6] and aerospace [7] in which compactness and high precision are fundamental. As highlighted in [8], strain wave gears are subjected to peculiar fault and failure modes that must be taken into account for a proper design and implementation of such technology.

Through a first-approximation multibody model [9], the present paper describes a preliminary representation of the dynamics of a strain wave gear in an EMA for eVTOL flight control systems. With the aim of providing the basis for the definition of future PHM algorithms, the kinematic error, modelled according to a physics-based approach [10], has also been considered in the simulation environment to study its influence on the performance of a flight control actuator.

Dynamic Model of an EMA for eVTOL Aircraft

Even though eVTOL aircrafts are based on a specific design [11], they are very similar in almost all their configurations from an actuation point of view. In this paper, the actuator analyzed is the one that allows obtaining a vectoring of the thrust device to change from take-off to cruise configuration. The specific aim of the present model is to study the effect of the kinematic error of the strain wave gear. For this reason, all the components of the EMA, except the gearbox, are represented using simplified models. The three main elements of the model are the Electric Motor (EM) and its control logic, the strain wave gear, and the sensors. As in the real system, the only input to the model is the position set value required by the flight control computer. All the other quantities (i.e., motor voltage and current, angular velocity, and torque) are internally calculated according to the classic EMA scheme [12].

Electric Motor. To build a high-fidelity model of a mechanical system, all its components must be properly modelled. However, since this would lead to high simulation times, simplifications have been adopted. Within this framework, in the present research, a model of a DC brushless motor has been implemented.

Strain Wave Gear. To describe the kinematic and the dynamic behaviour of the SWG, an equivalent model is exploited. This model is a good compromise between the need for high-fidelity representation and limited simulation time. The proposed model is based on the work done in [9], in which, the interactions among the three main components of the SWG were analysed.

This approach allows describing the cyclic deformation of the flexspline caused by the motion of the Wave Generator (WG) and the interaction during the meshing between the flexspline (FS) and circular spline (CS) teeth. The operating mode of a SWG can be dual, depending on which element, between the FS and the CS, is locked. In the present paper, the FS is fixed, while the CS is connected to the output shaft.

Differently from [9], the mechanical transmission between the electric motor shaft and the WG and between the CS and the position transducer have been considered. In so doing, it is possible to obtain a three degree-of-freedom model distinguishing the three inertias, one for each main component of the SWG.

In Figure 1.a a schematic representation of the equivalent model is reported. The physical and geometric parameters associated with it are the primitive equivalent radius (r_g), the wave generator angular position (θ_{WG}), the circular spline angular position (θ_{CS}), the teeth pressure angle (α_t), the elliptical cam equivalent angle ($\alpha_n = \arctan\left(\frac{1}{\tau * \tan(\alpha_t)}\right)$), the stiffness ($K_b$) and the viscous damping coefficient (c_b) of the elliptical bearing, the flexspline torsional stiffness (K_t), the meshing stiffness between FS and CS (K_m) and the pure kinematic error between input and output of the strain wave gear (θ_e). The displacements of the components that occur during the transmission are the radial displacement of the bearing outer race (x_1), the radial displacement of

Materials Research Proceedings **26** (2023) 207-212 https://doi.org/10.21741/9781644902431-34

the FS during elliptical deformation (x_2), the tangential displacement of the FS free edge caused by torsional deformation (y_1) and the tangential displacement of the CS (y_2).

By analyzing the free-body diagrams of the single components, it is possible to obtain the equations (Eq. 1) describing the dynamics of the system.

$$\begin{cases} T_{WG} = K_{WG}(\theta_{in} - \theta_{WG}) + c_{WG}\left(\dot{\theta}_{in} - \dot{\theta}_{WG}\right) = T_{FS\to WG} + J_{WG}\ddot{\theta}_{WG} \\ F_b = K_b\left(e_{WG,mis} + x_1 - x_2\right) + c_b(\dot{e}_{WG,mis} + \dot{x}_1 - \dot{x}_2) \\ F_b - \frac{J_{FS}\ddot{x}_2}{r_g^2} = F_m \sin(\alpha_t) \\ \frac{K_t y_1}{r_g^2} + \frac{c_t \dot{y}_1}{r_g^2} = -\frac{J_{FS}\ddot{y}_1}{r_g^2} + F_m \cos(\alpha_t) \\ F_m = K_m(x_2 \sin(\alpha_t) - (y_1 + y_2)\cos(\alpha_t)) + c_m(\dot{x}_2 - (\dot{y}_1 + \dot{y}_2)\cos(\alpha_t)) \\ T_{FS\to CS} - J_{CS}\ddot{\theta}_{CS} = K_{CS}(\theta_{CS} - \theta_{out}) + c_{CS}\left(\dot{\theta}_{CS} - \dot{\theta}_{out}\right) = T_{CS} \\ T_{FS\to WG} = F_b r_g \sin(\alpha_n)\cos(\alpha_n) \\ T_{FS\to CS} = F_m r_g \cos(\alpha_t) \end{cases} \quad (1)$$

The equations were implemented in a Simulink model to obtain a description of the SWG dynamics.

Kinematic error. The kinematic error is always present in SWGs, due to the FS flexibility, tolerances, and tooth machining errors. It is defined as:

$$\tilde{\theta} = \frac{\theta_{in}}{\tau} - \theta_{out} = (\theta_{CS} + \theta_e + \Delta\theta) - \theta_{out} = \theta_e + \Delta\theta \quad (2)$$

The term $\Delta\theta$ of the Eq. 2 is related to the torsional compliance, while θ_e is called pure kinematic error [13] and it depends on the kinematic structure of the SWG. The parameter $e_{WG,mis} = \theta_{e,mis} r_g \cong \theta_e r_g$ is the kinematic error caused by misalignment expressed as a radial displacement.

The pure kinematic error contributions can be classified into a constant component, related to clearance, and a variable one, related to misalignment and tooth machining error [10]. In [9,14,15], the presence of the kinematic error is modelled by means of finite Fourier series based on experimental data. On the contrary, the present study aims to describe such a phenomenon from its root causes such as a misalignment of the wave generator due to assembly and machining imperfections.

The modelling of the presence of misalignment among the three main components of the SWG is obtained by means of a roto-translation matrix depending on the wave generator angular position. In this way, it is possible to define a planar equivalent WG profile, depicted in Figure 1.b, changing, at each instant, with the input shaft position.

The input parameters of the kinematic error model are the eccentricity (e_1 and e_2) and the angular deviations ($\bar{\beta} = [\beta_1 \beta_2 \beta_3]$ and $\bar{\alpha} = [\alpha_1 \alpha_2 \alpha_3]$) shown in Figure 2.

Materials Research Proceedings **26** (2023) 207-212 https://doi.org/10.21741/9781644902431-34

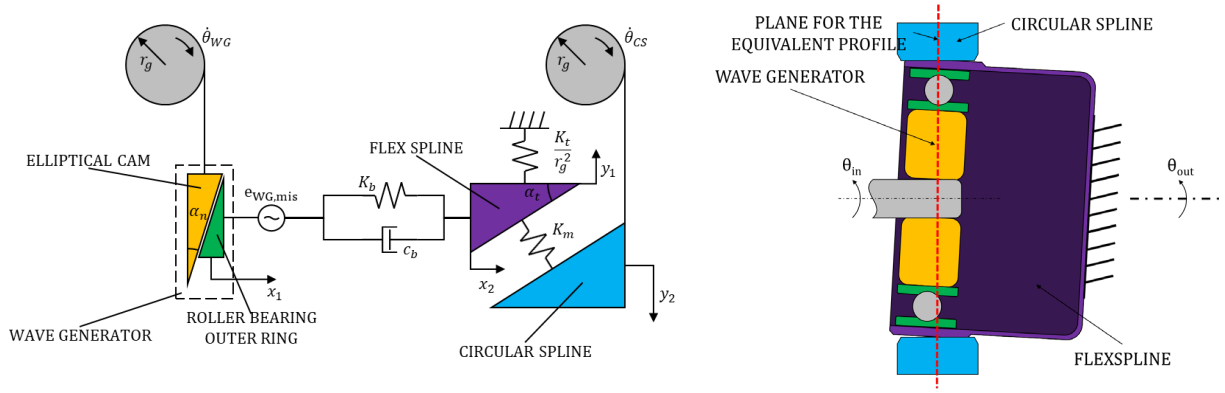

Figure 1 (a) Diagram of the SWG dynamic equivalent model. (b) Schematic representation of a misaligned strain wave gear.

The two eccentricity values are measured, respectively, between the CS center (O_{CS}) and the nominal center of the reference frame (O), and between the nominal center (O) and the WG center (O_{WG}). The angular deviations are the angles between eccentricities (e_1 and e_2) and x-axes (β_1 and α_1), between CS Z-axis and nominal Z-axis, nominal Z-axis and WG Z-axis on XOZ-plane (β_2 and α_2) and between CS Z-axis and nominal Z-axis, nominal Z-axis and WG Z-axis on YOZ-plane (β_3 and α_3). By knowing these parameters, it is possible to define two rotation matrices linking the nominal position of the WG to its angular position in presence of misalignment.

The obtained 3D profile of the wave generator is intersected with the plane perpendicular to the input shaft obtaining its equivalent planar profile. This is compared to the nominal one to get the radial displacement and, as a direct consequence, the kinematic error associated with it. In Figure 3.a, a comparison of the pure kinematic error between experimental [13] and proposed model simulated data is reported.

For more accurate results, proper modelling of the other kinematic error sources, such as clearance and tooth machining error, is necessary.

Friction. Due to the presence of friction, a passive torque, modeled by an approximation of the Stribeck curve as in [12], must be subtracted to T_{CS}, the output torque of the circular spline, to obtain the actual torque (T) at the output shaft of the reducer [16].

Sensors. Before being used to close the relative control loops, the signals of the flap surface angular position, the motor angular velocity and current pass-through blocks simulating the presence of three sensors. Zero-order transfer functions have been adopted to simulate the current sensors, while first and second-order ones have been implemented for the speed and the position sensors. In addition, to replicate a real device, noise has been added.

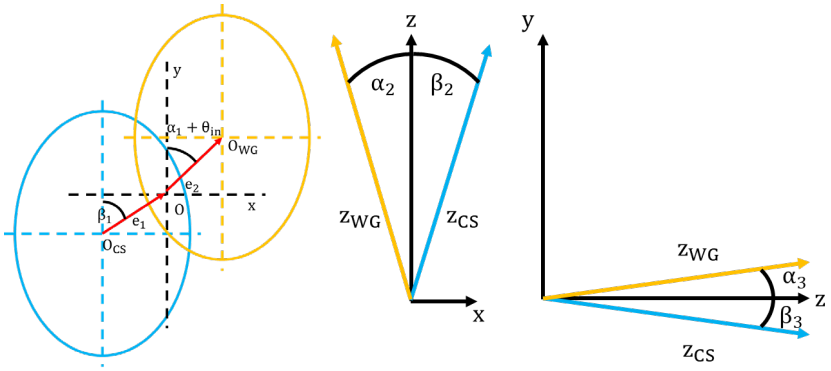

Figure 2 Eccentricity and angular deviations.

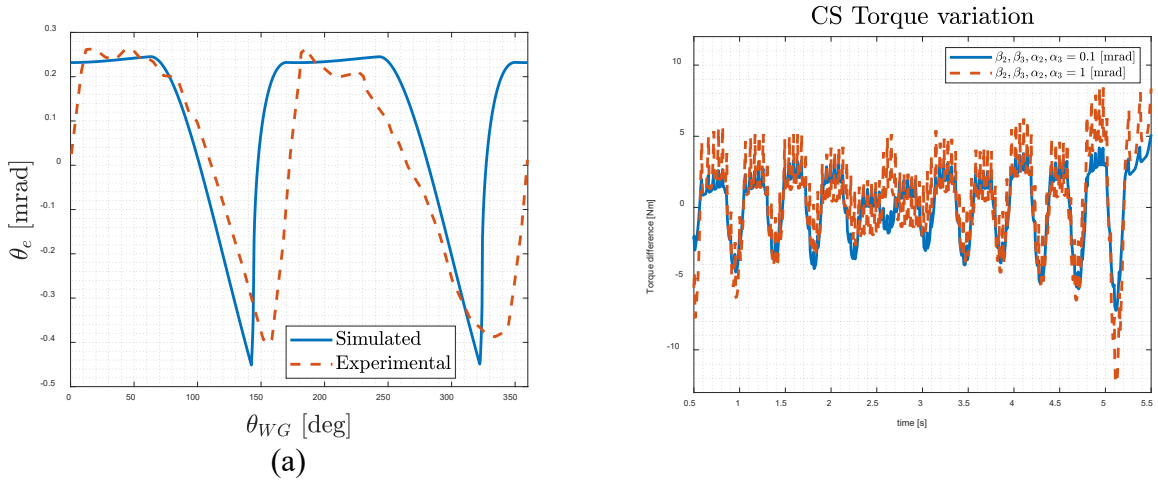

(a)

Figure 3 Analysis of the kinematic error model: (a) comparison of the pure kinematic error between experimental and simulated data and (b) angular deviation misalignment kinematic error.

Simulations Results

To study the effect of the presence of the kinematic error caused by misalignment, different simulations, performed by changing the input parameters (eccentricity, e_1 and e_2, and angular deviations, $\bar{\beta}$ and $\bar{\alpha}$), were run.

The angular position set is a ramp with a slope such that the maximum stroke of the actuator is reached in 5 s. In so doing, the speed of the actuator is constant, and the torque oscillations are primarily linked to the control logic. The simulations are performed by analyzing the effects of angular deviations ($\bar{\beta}$ and $\bar{\alpha}$). Because the position control loop operates to minimize the relative error the effect of the kinematic error on the flap surface angular position is negligible. Nevertheless, an effect could be observed in torques, and consequentially, in current signal, as reported in Figure 3.b in which the presence of the kinematic error caused a noisy signal with several oscillations. In Figure 3.b, are reported the differences between the nominal torque and the one in the presence only of angular deviations. As predictable, the effect of the kinematic error increases together with the misalignment level. A similar effect can be found in presence of misalignments.

Conclusions

In the present paper, a preliminary study on the effects of a strain wave gear pure kinematic error in an electro-mechanical actuator for UAM applications was proposed. For this purpose, a mathematical model of the SWG and relative misalignment was developed to study and quantify the effects on the main signals of the EMA.

In the analyzed case study, the results of the simulation made it possible to investigate one of the causes of vibrations between the components of a SWG. The presence of this error causes the appearance of oscillating torques which are instantaneously significantly greater than the nominal ones.

In the future, the proposed model will be validated with experimental results and integrated with more accurate ones of the other components of the EMA to study the effects of different phenomena and to obtain datasets suitable for PHM purposes.

References

[1] Ranasinghe, K., Sabatini, R., Gardi, A., Bijjahalli, S., Kapoor, R., Fahey, T., and Thangavel, K., Advances in Integrated System Health Management for Mission-Essential and Safety-Critical Aerospace Applications, Prog. Aerosp. Sci., 128 (2021), p. 100758. https://doi.org/10.1016/j.paerosci.2021.100758

[2] De Martin, A., Jacazio, G., and Vachtsevanos, G., Anomaly Detection and Prognosis for Primary Flight Control EMAs, European Conference of the Prognostic and Health Management Society, Bilbao, 2016, pp. 1–9.

[3] Bertolino, A. C., Sorli, M., Jacazio, G., and Mauro, S., Lumped Parameters Modelling of the EMAs' Ball Screw Drive with Special Consideration to Ball/Grooves Interactions to Support Model-Based Health Monitoring, Mech. Mach. Theory, 137 (2019) pp. 188–210. https://doi.org/10.1016/j.mechmachtheory.2019.03.022

[4] Bertolino, A. C., De Martin, A., Mauro, S., and Sorli, M., Multibody Dynamic Adams Model of a Ball Screw Mechanism with Recirculation Channel, ASME Int. Mech. Eng. Congr. Expo. Proc., (2021). https://doi.org/10.1115/IMECE2021-71121

[5] Bacci, A., Bertolino, A. C., De Martin, A., and Sorli, M., Multiphysics Modeling of a Faulty Rod-End and Its Interaction with a Flight Control Actuator to Support Phm Activities, ASME Int. Mech. Eng. Congr. Expo. Proc., (2021) pp. 1–10. https://doi.org/10.1115/IMECE2021-71095

[6] Li, Z., Melek, W. W., and Clark, C., Decentralized Robust Control of Robot Manipulators with Harmonic Drive Transmission and Application to Modular and Reconfigurable Serial Arms, Robotica, 27(2) (2021) pp. 291–302. https://doi.org/10.1017/S0263574708004712

[7] Ueura, K., Kiyosawaa, Y., Kurogi, J., Kanai, S., Miyaba, H., Maniwa, K., Suzuki, M., and Obara, S., Tribological Aspects of a Strain Wave Gearing System with Specific Reference to Its Space Application, Proc. Inst. Mech. Eng. Part J J. Eng. Tribol., 2008. https://doi.org/10.1243/13506501JET415

[8] Raviola, A., Martin, A. De, Guida, R., Jacazio, G., Mauro, S., and Sorli, M., Harmonic Drive Gear Failures in Industrial Robots Applications : An Overview, European Conference of the Prognostic and Health Management Society, 2021, pp. 350–360.

[9] Zhang, X., Tao, T., Jiang, G., Mei, X., and Zou, C., A Refined Dynamic Model of Harmonic Drive and Its Dynamic Response Analysis, Shock Vib., (2020). https://doi.org/10.1155/2020/1841724

[10] Jia, H., Li, J., Xiang, G., Wang, J., Xiao, K., and Han, Y., Modeling and Analysis of Pure Kinematic Error in Harmonic Drive, Mech. Mach. Theory, 155 (2021). https://doi.org/10.1016/j.mechmachtheory.2020.104122

[11] Bacchini, A., and Cestino, E., Electric VTOL Configurations Comparison, Aerospace, 6(3) (2019). https://doi.org/10.3390/aerospace6030026

[12] Guida, R., Raviola, A., Migliore, D. F., De Martin, A., Mauro, S., and Sorli, M., Simulation of the Effects of Backlash on the Performance of a Collaborative Robot: A Preliminary Case Study, 31st International Conference on Robotics in Alpe-Adria-Danube Region, Klagenfurt am Wörthersee, 2022, pp. 28–35. https://doi.org/10.1007/978-3-031-04870-8_4

[13] Ghorbel, F. H., Gandhi, P. S., and Alpeter, F., On the Kinematic Error in Harmonic Drive Gears, J. Mech. Des. Trans. ASME, 123(1) (2001) pp. 90–97. https://doi.org/10.1115/1.1334379

[14] Preissner, C., Royston, T. J., and Shu, D., A High-Fidelity Harmonic Drive Model, J. Dyn. Syst. Meas. Control. Trans. ASME, 134(1) (2012). https://doi.org/10.1115/1.4005041

[15] Zou, C., Tao, T., Jiang, G., Mei, X., and Wu, J., A Harmonic Drive Model Considering Geometry and Internal Interaction, Proc. Inst. Mech. Eng. Part C J. Mech. Eng. Sci., 231(4), 2017, pp. 728–743. https://doi.org/10.1177/0954406215621097

[16] Ma, D., Yan, S., Yin, Z., and Yang, Y., Investigation of the Friction Behavior of Harmonic Drive Gears at Low Speed Operation, Proceedings of 2018 IEEE International Conference on Mechatronics and Automation, ICMA 2018, IEEE, (2018) pp. 1382–1388. https://doi.org/10.1109/ICMA.2018.8484324